Journal of Catalysis 257 (2008) 270–282

Contents lists available at ScienceDirect

Journal of Catalysis

www.elsevier.com/locate/jcat

Role of ammonia in the reduction by hydrogen of NO_x stored over Pt–Ba/Al_2O_3 lean NO_x trap catalysts

Luca Lietti *, Isabella Nova, Pio Forzatti

Politecnico di Milano, Dipartimento di Energia, Laboratory of Catalysis and Catalytic Processes and Centro NEMAS – Nano Engineered MAterials and Surfaces, P.zza L. Da Vinci 32, 20133 Milano, Italy

ARTICLE INFO

Article history:
Received 14 September 2007
Revised 30 April 2008
Accepted 3 May 2008
Available online 5 June 2008

Keywords:
Lean deNO_x
NO_x reduction mechanism
LNT systems
Pt–Ba/Al_2O_3 catalyst
Transient response method

ABSTRACT

The reduction by H_2 of nitrates stored on a model Pt–Ba/Al_2O_3 catalyst under isothermal conditions was investigated. An in-series two-step process involving at first the formation of ammonia on reaction of nitrates with H_2 (step 1), followed by the reaction of ammonia with residual stored nitrates to give N_2 (step 2) is proposed. Different temperature thresholds for the two steps are identified, with step 1 being much faster than step 2. The reaction of ammonia with nitrates to give nitrogen (step 2) is very selective, is rate-determining, and represents the major route for nitrogen formation. Due to the fast reduction of adsorbed nitrates by hydrogen (step 1) and to the "plug-flow" integral behavior of the reactor, an H_2 front develops that travels along the reactor. Ammonia is readily produced at the front; if the temperature is high enough, then the regeneration process continues downstream of the hydrogen front due to the reaction of NH_3 with the stored nitrates, leading to N_2 production. This fully explains the change in product distribution with time observed at the reactor outlet during regeneration of LNT catalysts, as well as the effect of temperature on the selectivity of the process. The effects of water and CO_2 on the reduction process also are addressed. Water favors the first step of the reduction process but has no significant impact on the subsequent reaction of ammonia with stored nitrates, whereas CO_2 has a strong inhibiting effect both on the reduction of nitrates to ammonia by H_2 (step 1) and on the subsequent reaction of ammonia with the residual stored nitrates (step 2), due to poisoning of Pt by CO.

1. Introduction

The reduction of NO_x emission from lean-burn engines has been the subject of several studies. So far, two different solutions have been applied at a commercial scale: the NH_3- or urea-SCR (selective catalytic reduction) process and the NO_x storage-reduction (NSR) technique. The NH_3-SCR technique is well established for stationary sources [1]; the activity and selectivity, along with the resistance to catalyst poisoning and aging, have made the NH_3-SCR process very appealing for complying with future NO_x emission standards for vehicles. In 2005, most European truck producers launched urea-SCR equipped trucks able to meet the Euro 4 and Euro 5 emission standards [2–4]. Presently the SCR technology is also under evaluation for passenger cars. The great potential of the SCR system is counterbalanced by the complex vehicle exhaust layout and cost (due to the urea tank, sensors, dosing system, injector, mixer, etc.), which may limit a possible SCR application to high-segment vehicles.

The NSR technique (also known as NO_x adsorbers or lean NO_x traps [LNT]) was specifically developed for mobile sources and launched on the market by Toyota in the 1990s [5,6], but also has been proposed for stationary gas turbines [7]. Basically, LNTs consist of an alumina support on which an alkali- or alkali-earth metal oxide (e.g., Ba) and a noble metal (Pt) are deposited. These catalysts operate under cyclic conditions. During the lean period, NO_x is stored on Ba, whereas during the subsequent short, rich phase, the adsorbed NO_x species are reduced to nitrogen on Pt. An advantage of this technology with respect to the SCR technique is that LNTs do not make use of an ammonia precursor as a reductant, so that no relevant layout modifications are needed; accordingly LNT could be considered a complementary tool, applicable on low-segment vehicles [3,4]. The resistance to thermal aging and sulfur poisoning of NSR catalysts remain to be improved, however. Moreover, although these catalysts are being used on a commercial scale, detailed knowledge of their behavior and of the chemical pathways governing both the storage of NO_x species and their reduction remains lacking [8].

More recently, combined LNT-SCR systems also have been proposed in which the NO_x stored on the LNT catalyst are reduced to ammonia, which then is produced on board and used as a reactant in the SCR system [9].

The mechanism governing the reduction of the stored NO_x is not well understood. There is now a general consensus on the fact

* Corresponding author.
E-mail address: luca.lietti@polimi.it (L. Lietti).

0021-9517/$ – see front matter
doi:10.1016/j.jcat.2008.05.005

that the regeneration of NSR catalysts implies at first the release of NO_x in the gas phase from the alkali- or alkali-earth metal compound, followed by the reduction of the released NO_x to N_2 and other products, including ammonia [8].

The mechanisms leading to the release of NO_x in the gas phase and their subsequent reduction remain under debate. It has been proposed that the NO_x release is driven by heat generated from the reducing switch (thermal release) [10,11] and/or by the establishment of a net reducing environment, which decreases the thermodynamic stability of nitrates [12–15]. Other studies carried out under isothermal conditions suggested the existence of a Pt-catalyzed pathway involving H_2 activation, followed by surface spillover toward nitrate adspecies that decompose to gaseous NO_x [12,16–19]. The routes responsible for the reduction of the evolved NO_x to N_2 (and other products) have not been completely clarified to date, although it has been argued that the reduction of NO_x in rich and/or stoichiometric environments occurs according to the well-established chemistry and mechanisms of three-way catalysts. In this respect, proposed mechanisms include (i) the NO decomposition on reduced Pt sites (the role of the reductant in this mechanism is to kept Pt in a reduced form) [20] and (ii) the direct reaction between released NO_x species and the reductant molecule on the precious metal sites [21]. But these mechanisms can hardly explain both the very high N_2 selectivity and the temporal sequence of products (with ammonia detection following that of nitrogen) seen on regeneration of LNT systems with hydrogen used as a reductant under isothermal conditions.

Cumaranatunge et al. [22] recently proposed a simplified scheme for the reduction of the stored NO_x by H_2. In particular, these authors provided evidence for the development of a reaction front that travels along the trap during the regeneration stage. Ammonia and N_2 can be formed simultaneously in the H_2-rich zone of the front, according to previously suggested mechanisms for three-way catalysts; however, NH_3 may react further with the stored nitrates, leading to the formation of N_2. This would explain the temporal sequence of the product formation, with NH_3 breakthrough observed after N_2 production when the stored NO_x starts to become depleted and is insufficient to react with the NH_3 formed upstream. A similar scheme also has been proposed by Pihl et al. [23].

To gain further insight into the mechanism governing the reduction of the stored NO_x and on the role of NH_3 in the process, we analyzed the reactivity toward H_2 and NH_3 of NO_x stored over a model Pt–Ba/γ-Al_2O_3 catalyst. For this purpose, NO_x was adsorbed on the catalyst surface at 350 °C from NO/O_2, after which the reactivity of the stored NO_x with H_2 and NH_3 was investigated using both temperature-programmed surface reaction (TPSR) and the isothermal transient response method (ITRM). Reduction of the stored NO_x was accomplished in both the presence and absence of water and of CO_2 in the feed stream, to clarify the effect of such species on the reduction mechanism and on the reactivity of the stored NO_x. Eventually, complete characterization of the reactivity of the stored NO_x was attained, and a reaction pathway operating in the regeneration of LNT systems under isothermal conditions was identified.

2. Methods

2.1. Materials

The model Pt–Ba/γ-Al_2O_3 (1/20/100 w/w) sample used in this study was prepared by impregnating a binary Pt/γ-Al_2O_3 sample with an aqueous solution of $Ba(CH_3COO)_2$ (Strem Chemical, 99%), followed by exsiccation at 80 °C and calcination at 500 °C for 5 h. The Pt/γ-Al_2O_3 was obtained by impregnating a γ-Al_2O_3 carrier, calcined at 700 °C (Versal 250; La Roche Chemicals; surface area of 200 m^2/g and pore volume of 1.2 cm^3/g after calcination at 700 °C), with a solution of $Pt(NH_3)_2(NO_2)_2$ (Strem Chemicals, 5% Pt in ammonium hydroxide), followed by exsiccation at 80 °C overnight and calcination at 500 °C for 5 h [24]. The impregnation order of first Pt, followed by Ba was adopted to ensure good dispersion and stability of the noble metal on the alumina support, in line with the recipes of Toyota patents [25].

2.2. Apparatus and procedures

The NO_x adsorption–reduction tests were performed in a quartz tubular fixed-bed microreactor using 60 mg of catalyst (100–150 μm). The reactor outlet was connected to a mass spectrometer for complete analysis of reactants and products [24,26,27]. Before each test, the catalyst samples were conditioned by performing a few adsorption/regeneration cycles with NO/O_2 (1000 ppm NO and 3% v/v O_2 in He) and H_2 (2000 ppm in He) at 350 °C, with an inert purge (He) between the two phases. Conditioning was done until a reproducible behavior was obtained, which typically required 2 or 3 cycles.

After catalyst conditioning at 350 °C, NO_x was adsorbed at the same temperature. This was accomplished by imposing a rectangular step feed of NO (1000 ppm) in flowing He + 3% v/v O_2, followed by a He purge at the same temperature to provoke the desorption of weakly adsorbed species. The length of the NO_x adsorption phase was selected to store about 3×10^{-4} mol/g_{cat} of NO_x on the catalyst surface.

The reduction of the adsorbed NO_x species was performed with both H_2 and with NH_3 according to different procedures: TPSR and ITRM. In the first case (TPSR experiment), during the He purge after NO_x adsorption, the catalyst was cooled to room temperature (RT), and then a rectangular step feed of H_2 (2000 ppm in He) was admitted to the reactor at the same temperature. When the mass-spec signals were stabilized, the catalyst temperature was linearly increased from RT to 500 °C (at a heating rate of 10 °C/min) while monitoring the concentration of the products exiting the reactor.

In the ITRM experiments, reduction of the stored nitrates was carried out at constant temperature in the range 100–350 °C. Accordingly, during the He purge after NO_x adsorption, the catalyst temperature was set at the desired value, and then, after stabilization of the mass-spec signals, a rectangular step feed of H_2 (2000 ppm in He) or NH_3 (1000 ppm in He) was admitted to the reactor, resulting in reduction of the stored nitrates. Notably, due to the low concentration of the reductant, the reduction process was not accompanied by significant thermal effects; that is, reduction of the stored nitrates was carried out under nearly isothermal conditions [16]. When the reduction process was completed (i.e., when the concentration of the products exiting the reactor was negligible), the H_2 or NH_3 flow was stopped, and the catalyst was heated to 350 °C under He flow. Eventually a new H_2 step (2000 ppm in He) was fed to the reactor at 350 °C to complete the reduction of the residual amounts of nitrates remaining after the previous reduction treatment, if any. This procedure allowed us to quantify the extent of nitrate reduction during the rich phase at each temperature (efficiency in the reduction of the stored NO_x). A flow of 100 cm^3/min (@ 1 atm and 0 °C) was used for all experiments. The N-balance, estimated by comparing the amounts of NO_x adsorbed during the lean phase with those of the N-containing species formed on reduction of the stored NO_x, always closed within ±5%.

When H_2 was used as a reductant, the selectivity to N_2 of the reduction process could be estimated. Of note, because the concentration of the reduction products (N_2, NO, and NH_3) changed with time during the reduction phase, the selectivity also changed with time. Accordingly, the time-weighted average N_2 selectivity of the reduction process (S_{N_2}) was estimated. Calculation was carried out

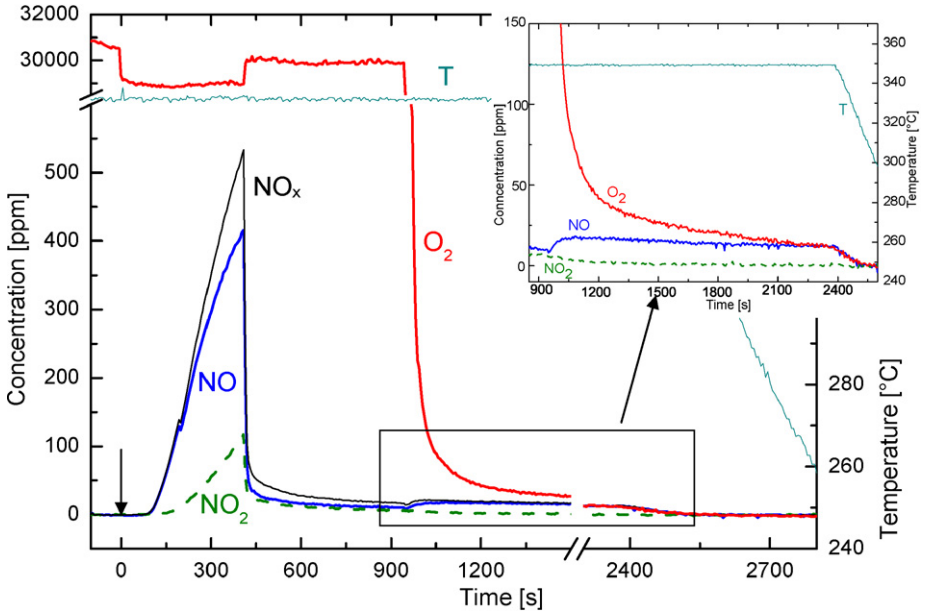

Fig. 1. Temporal evolution of NO, NO_2 and NO_x ($NO + NO_2$) outlet concentrations upon adsorption of NO (1000 ppm) in $He + O_2$ 3% v/v at 350 °C over the Pt–Ba/γ-Al_2O_3 catalyst.

from the total molar amounts of N_2, NO, and NH_3 (n_{N_2}, n_{NO} and n_{NH_3}, respectively) evolved during the entire reduction phase,

$$S_{N_2} = \frac{2n_{N_2}}{2n_{N_2} + n_{NO} + n_{NH_3}}. \quad (1)$$

N_2O concentration was always negligible in the experiments; accordingly, this species is not included in Eq. (1). When NH_3 was used as a reductant, the selectivity to N_2 was always complete, because only nitrogen was observed among the reaction products.

The role of water and of CO_2 in the reduction also was investigated by performing TPSR and ITRM experiments in the presence of water and of both H_2O and CO_2 (1% v/v and 3000 ppm, respectively). These species were present during the regeneration step only, whereas NO_x adsorption always was carried out from NO in He/O_2.

3. Results and discussion

3.1. NO_x storage at 350 °C

Fig. 1 presents a typical result obtained on NO adsorption in $He + O_2$ at 350 °C over the Pt–Ba/γ-Al_2O_3 catalyst. Here NO was admitted to the reactor at $t = 0$ s (arrow in Fig. 1); after 100 s, NO breakthrough was observed, whereas NO_2 evolution was seen starting at 150 s. Both the NO and NO_2 outlet concentrations increased with time until the NO feed flow was switched off ($t =$ 400 s); after the switch, a tail in the NO and NO_2 profiles, due to the desorption of weakly adsorbed species, was observed. The desorption process was very slow; the NO and NO_2 concentrations were not yet decreased to zero after several minutes. An additional minor NO desorption was seen at $t \sim 900$ s after the oxygen flow was switched off (He purge), in line with the effect of oxygen partial pressure on the stability of nitrate species formed onto the catalyst surface [12,28]. Finally, at $t = 2400$ s, the NO concentration quickly dropped to zero when the catalyst temperature was decreased.

Of note, NO_x was stored primarily in the form of nitrates after this procedure, as pointed out by previous FTIR experiments [26]. The amounts of NO_x stored over the model Pt–Ba/Al_2O_3 catalyst after the He purge was close to 3×10^{-4} mol/g_{cat}, corresponding to an overall Ba utilization (i.e., the fraction of Ba involved in the storage by assuming the formation of $Ba(NO_3)_2$) close to 12%. The NO_x trapping efficiency during NO storage (i.e., the ratio of the stored NO_x to the amounts of NO admitted to the reactor) was close to 80%.

Finally, it is noteworthy that the admission of CO_2 and/or water to the reactor at 350 °C after NO_x adsorption at the same temperature during the He purge (in the case of the TPSR/ITRM experiments carried out in the presence of CO_2 and/or water) did not lead to any significant NO_x release (data not shown in the figure), indicating that the stored NO_x was stable at 350 °C even in the presence of CO_2 and water.

3.2. Reduction of stored nitrates by H_2

The reduction of NO_x stored at 350 °C was carried out with 2000 ppm of hydrogen in both H_2-TPSR and H_2-ITRM experiments. Because preliminary experiments demonstrated that the difference in reactivity of H_2 and NH_3 during the reduction of stored nitrates was greater in the presence of water, here we first present the data obtained in the presence of water.

Fig. 2 shows the results obtained in the H_2-TPSR and NH_3-TPSR experiments carried out in $He + 1\%$ v/v H_2O. In the H_2-TPSR study (Fig. 2A), H_2 was consumed already at 50 °C; its concentration showed a minimum of 80 ppm near 100 °C and then slowly increased to the inlet value of 2000 ppm. Formation of reaction products can be seen starting at 65 °C with the evolution of ammonia along with very small amounts of N_2. Water (not shown in the figure) also was formed during reduction of the stored nitrates, in addition to that already present in the feed stream. Neither NO nor N_2O was detected in appreciable amounts during the TPSR run.

The data shown in Fig. 2A indicate that nitrates stored at 350 °C could be reduced by H_2 already at very low temperatures, leading to the formation of ammonia along with minor amounts of N_2. The high reactivity of H_2 toward nitrates and the very high selectivity to NH_3 are noteworthy. The overall H_2 consumption and the corresponding NH_3 and N_2 formation observed during the TPSR run are in line with the stoichiometry of the following reactions:

$$Ba(NO_3)_2 + 8H_2 \rightarrow 2NH_3 + Ba(OH)_2 + 4H_2O \quad (2)$$

and

$$Ba(NO_3)_2 + 5H_2 \rightarrow N_2 + Ba(OH)_2 + 4H_2O, \quad (3)$$

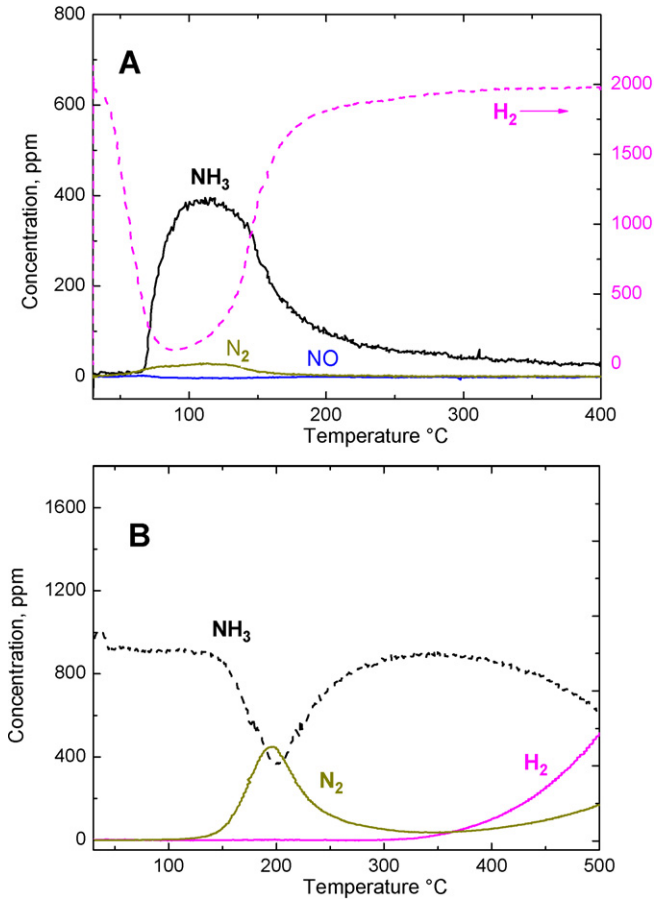

Fig. 2. H_2-TPSR (2000 ppm + 1% v/v H_2O in He) (A) and NH_3-TPSR (1000 ppm + 1% v/v H_2O in He) (B) after NO/O_2 adsorption at 350 °C over the Pt–Ba/γ-Al_2O_3 catalyst.

with reaction (2) accounting for more than 95% of the overall H_2 consumption.

In reactions (2) and (3), formation of $Ba(OH)_2$ is envisaged; as pointed out previously [24], $Ba(OH)_2$ is formed in a wet environment on reduction of the nitrates, although small amounts of BaO also may be present due to the reaction,

$$Ba(OH)_2 \rightarrow BaO + H_2O. \quad (4)$$

But this reaction does not affect the $H_2/Ba(NO_3)_2$ stoichiometric ratio of reactions (2) and (3) and the corresponding formation of NH_3 and N_2.

Notably, H_2 uptake is seen before the evolutions of the reaction products (ammonia): this suggests that H_2 is at first adsorbed and activated on the catalyst surface, and then participates in the reduction of nitrates. Nevertheless, a delay in the detection of ammonia due to its slow desorption from the catalysts surface cannot be excluded.

The nitrates stored at 350 °C also were reduced under isothermal conditions at different temperatures, in the range 100–350 °C (H_2-ITRM). Fig. 3 displays the concentration profiles of hydrogen, nitrogen, ammonia, and NO as a function of time. Fig. 4 displays the efficiency in the reduction of the stored NO_x (i.e., the fraction of NO_x stored at 350 °C that is reduced during the regeneration) and the overall N_2 selectivity of the reduction process (i.e., the time-weighted average selectivity of the reduction, Eq. (1)) calculated from the data in Fig. 3 as a function of the reduction temperature.

The lowest investigated temperature (100 °C) corresponds roughly to the minimum H_2 concentration seen during the H_2-TPSR experiment (Fig. 2A). At this temperature, a small, sharp H_2

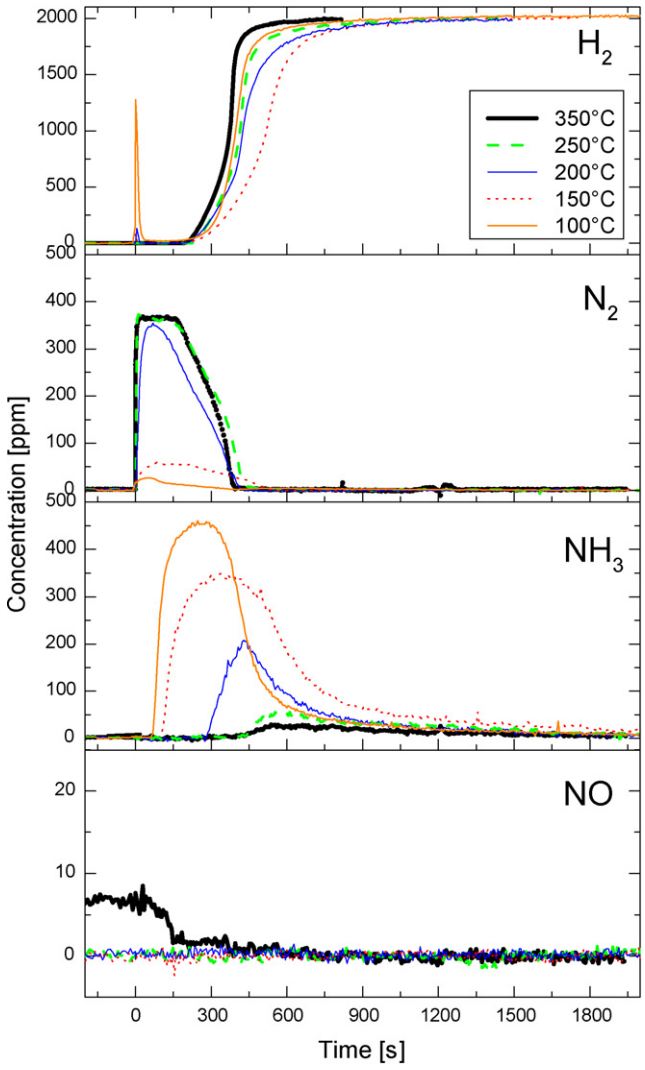

Fig. 3. Temporal evolution of H_2, N_2, NH_3 and NO outlet concentrations during reduction with H_2 (2000 ppm + 1% v/v H_2O in He) after NO/O_2 adsorption at 350 °C over the Pt–Ba/γ-Al_2O_3 catalyst (H_2-ITRM experiment).

peak is observed on the addition of H_2 at $t = 0$ s, followed by an almost complete uptake of H_2 (with the outlet H_2 concentration near 20 ppm). Eventually, after 200 s, the concentration increases up to the inlet value (2000 ppm). Large amounts of ammonia are detected at the reactor outlet in correspondence with H_2 consumption, although with a delay with respect to H_2 admission. Minor amounts of nitrogen also are formed, whereas no appreciable amounts of NO and N_2O are found at the reactor outlet; reaction (2) accounts for almost all of the H_2 consumption. These results are in line with those obtained in the H_2-TPSR experiments, demonstrating that the stored nitrates were reduced efficiently and selectively to ammonia already at very low temperatures. As a matter of fact, NO_x reduction efficiency >95% could be obtained at this temperature, whereas NH_3 formation accounts for >90% of the reaction products (with N_2 selectivity <10%; see Fig. 4B).

Significant changes in the product formation and in its temporal evolution are observed on increasing the reduction temperature of the nitrates stored at 350 °C. At 150 °C, the initial H_2 peak becomes negligible, and H_2 is completely consumed up to its breakthrough, near 220 s. N_2 formation increases slightly with respect to the reduction carried out at 100 °C, whereas that of NH_3 decreases, with an increasing delay in the evolution of ammonia. This leads to a

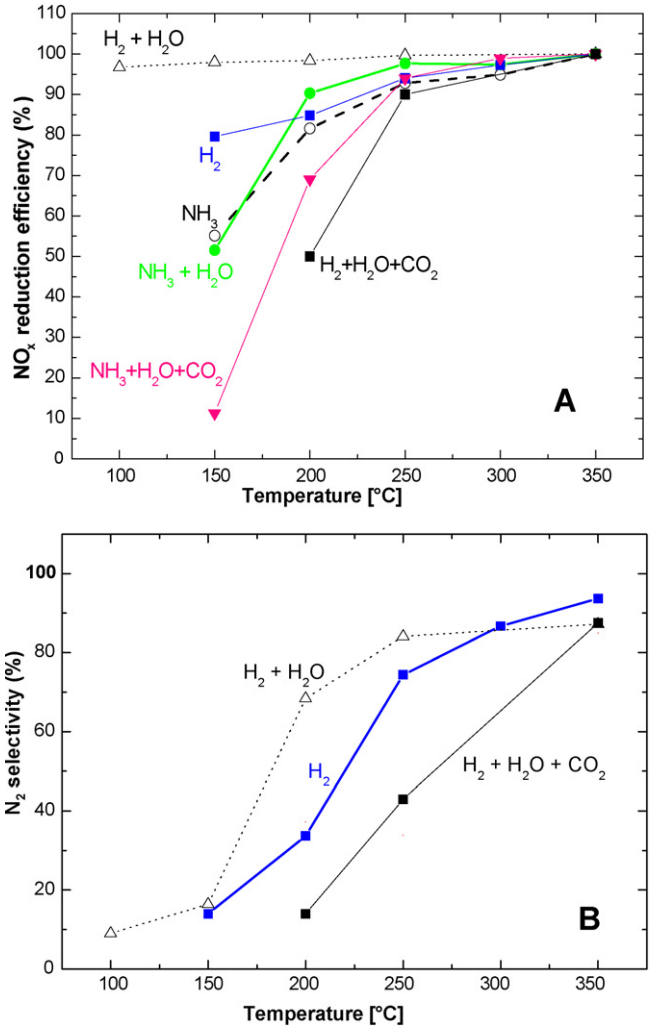

Fig. 4. NO_x reduction efficiency (A) and N_2 selectivity (B) upon reduction at different temperatures with various reducing mixtures after NO/O_2 adsorption at 350 °C over the Pt–Ba/γ-Al_2O_3 catalyst.

slight increase in N_2 selectivity (from 10% to 18%), with the NO_x reduction efficiency remaining very high (Fig. 4A).

A further increase in the reduction temperature (to 200 °C) favors N_2 formation at the expense of ammonia, resulting in increased N_2 selectivity (near 70%) at this temperature (see Fig. 4B). Moreover, the initial H_2 peak is no longer apparent. The N_2 selectivity increases further with increasing temperature, so that at the highest temperature investigated (350 °C), the stored NO_x are reduced primarily to N_2 (with N_2 selectivity near 90%). Notably, above 250 °C, the N_2 outlet concentration immediately increases to 370 ppm on H_2 admission; this concentration level closely corresponds to the stoichiometry of reaction (3) (i.e., to the reduction of nitrates by H_2). Above 250 °C, the reaction is very fast, and only minor amounts of NH_3 are found at the reactor outlet after the production of N_2. Accordingly, before the NH_3 breakthrough, complete selectivity to nitrogen is observed, if one neglects the small amounts of NO (in the order of few ppm) seen before H_2 admission due to the slow decomposition of the stored NO_x during the He purge (see Fig. 1). Moreover, no appreciable amounts of N_2O were observed at any temperature investigated.

Of note, whereas at the lowest temperatures investigated (100 and 150 °C), ammonia evolution precedes H_2 breakthrough, at higher temperatures, NH_3 evolution is seen together with or after H_2 breakthrough. This is accompanied by a change in the selectivity to N_2 with time at high T, from very high at the beginning of the reduction phase to very poor near the end, when ammonia is detected at the reactor outlet.

Our data indicate that the time-weighted average N_2 selectivity of the reduction process depends strongly on temperature. As shown in Fig. 4B, at low temperature, nitrates are reduced mainly to ammonia (with N_2 selectivity <10%). An increase in reduction temperature favors N_2 formation at the expense of ammonia, so that at high temperature (250 °C and above), N_2 is the most abundant reaction product. The observed dependence of the N_2 selectivity with temperature may suggest that the reduction of stored nitrates by H_2 occurs via a two-step pathway involving a first step, fast even at low temperatures, responsible for ammonia formation and hydrogen consumption, followed by a slower reaction of ammonia with residual nitrates to form nitrogen, occurring to a significant extent only at higher temperatures. To confirm these hypotheses, and specifically the reactivity of ammonia with nitrates in the formation of nitrogen, we performed NH_3-TPSR and NH_3-ITRM experiments after NO_x storage.

3.3. Reduction of stored nitrates by NH_3

Figs. 2B and 5 show the results of TPSR and ITRM experiments performed with NH_3 as a reductant, respectively. As in the case of H_2, nitrates were stored at 350 °C from a NO/O_2 mixture; reduction of the stored nitrates with NH_3 was carried out in the presence of H_2O (1% v/v). In the NH_3-TPSR experiment (Fig. 2B), ammonia is consumed starting from 130 °C; the NH_3 concentration shows a minimum of 400 ppm near 200 °C, returns to the inlet concentration value at 350 °C, and then decreases again at higher temperatures. Ammonia consumption is accompanied by N_2 formation below 350 °C and N_2 and H_2 evolution above 350 °C.

The ammonia consumption peak with minimum near 200 °C and the corresponding N_2 formation are due to the reduction of the stored nitrates by NH_3 according to the following overall stoichiometry:

$$3Ba(NO_3)_2 + 10NH_3 \rightarrow 8N_2 + 3Ba(OH)_2 + 12H_2O. \quad (5)$$

On the other hand, the decreased ammonia concentration seen at higher temperatures (above 350 °C) and the associated formation of N_2 and H_2 in a 1/3 ratio are related to the decomposition of ammonia,

$$2NH_3 \rightarrow N_2 + 3H_2. \quad (6)$$

Of note, as demonstrated by dedicated TPSR experiments carried out in the absence of stored nitrates, the temperature of the onset of ammonia decomposition is not affected by the presence of nitrates. Finally, it is noteworthy that neither NO nor N_2O was detected in appreciable amounts during the TPSR experiment.

Accordingly, the data demonstrate that above 130–150 °C, ammonia is an effective reductant for the stored nitrates and also is highly selective to nitrogen. However, the reactivity of NH_3 is markedly lower than that of H_2, which is able to reduce stored nitrates at temperatures as low as 60 °C (see Fig. 2A).

We also investigated the reactivity of ammonia in the reduction of stored nitrates through ITRM experiments, by feeding NH_3 at constant temperature (at 150–350 °C) in the presence of water (1% v/v) over the catalyst on which nitrates were previously adsorbed at 350 °C. The results of the NH_3-ITRM experiments are shown in Fig. 5. Fig. 4A illustrates the efficiency in the reduction of the stored NO_x calculated for the NH_3-ITRM experiments shown in Fig. 5; the data are compared with those obtained in the H_2-ITRM experiments discussed previously as well as with other data discussed below. As mentioned earlier, N_2 selectivity is always complete in this case.

When the reduction is carried out at 150 °C, the reactivity of ammonia in the reduction of the stored nitrates is very poor, in

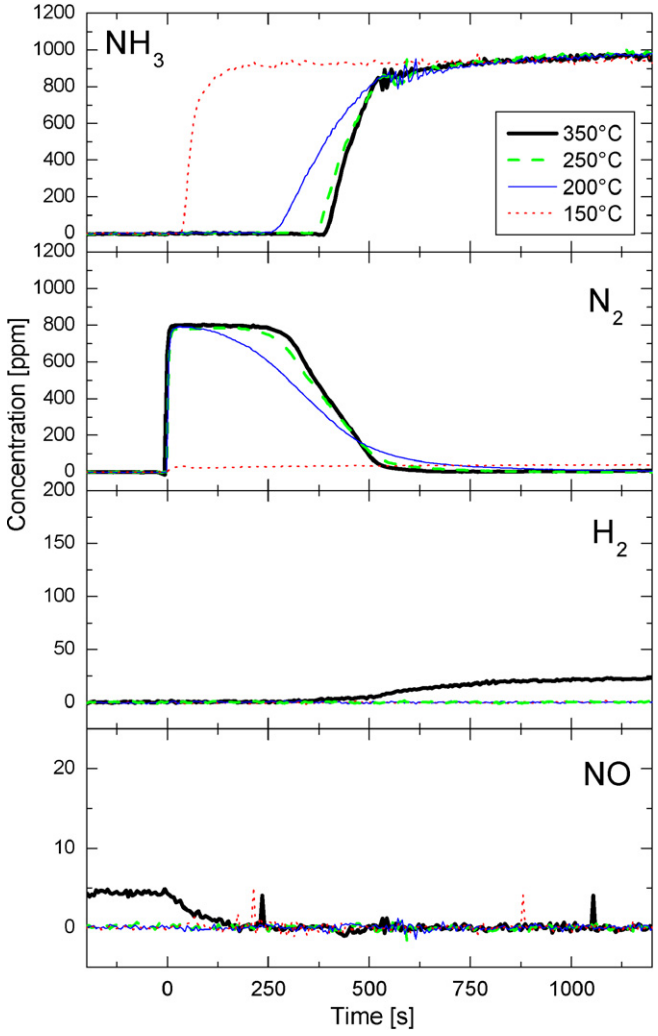

Fig. 5. Temporal evolution of NH_3, N_2, H_2 and NO outlet concentrations during reduction with NH_3 (1000 ppm + 1% v/v H_2O in He) after NO/O_2 adsorption at 350 °C over the Pt–Ba/γ-Al_2O_3 catalyst (NH_3-ITRM experiment).

line with TPSR data showing a temperature threshold for the reaction near 130–140 °C. Only minor amounts of N_2 (near 50 ppm) are detected after the addition of NH_3 at 150 °C, because the reaction is under kinetic control and is limited by the reactivity of ammonia. The reaction proceeds for nearly 1 h, after which the N_2 concentration drops to zero (data not shown). The overall amount of N_2 produced at the end of the reduction process (1.6×10^{-4} mol/g_{cat}) corresponds to the near 50% reduction of the initially adsorbed nitrates (Fig. 4A). This was confirmed by a subsequent treatment with H_2 at higher temperature (350 °C), which caused the reduction of the residual nitrates to nitrogen in comparable quantities (1.5×10^{-4} mol/g_{cat}). The overall amount of N_2 produced in the reduction is consistent with the amount of nitrates initially stored on the catalyst (near 3.1×10^{-4} mol/g_{cat}).

When the reduction temperature is increased to 200 °C, the stored NO_x are readily reduced to N_2; in fact, on the stepwise addition of NH_3 at $t = 0$ s, ammonia is completely consumed and the N_2 outlet concentration immediately increases to near 800 ppm. This concentration corresponds to that expected from the reduction of nitrates by NH_3 according to the stoichiometry of reaction (5). The reaction is very fast at this temperature (200 °C). The reaction rate is controlled by the inlet concentration of ammonia, and the reduction process is highly selective toward N_2; negligible amounts of N_2O and NO are seen.

After 100 s, the N_2 concentration starts to decrease, and at 250 s, the ammonia breakthrough is observed. Then the NH_3 concentration slowly increases to the inlet value while the N_2 concentration shows a prolonged tail, which extends up to 1000 s. Roughly 90% of the initially adsorbed nitrates are removed at this temperature.

On further increasing the reduction temperature (to 250 and 350 °C), the reaction becomes faster; the NH_3 breakthrough is shifted to 375 s and becomes very sharp. At the highest temperature investigated (350 °C), when the reduction process is complete (near 500 s), small amounts of H_2 (near 20 ppm) are found at the reactor outlet, due to ammonia decomposition. No N_2 is observed, because the expected concentration of this species (7 ppm) is near the detection limit of our apparatus. This is consistent with the results of the NH_3-TPSR experiment (Fig. 2B) showing the ammonia decomposition reaction above 350 °C. Neither NO nor N_2O formation is detected at these temperatures.

As shown in Fig. 4A, the NO_x reduction efficiency obtained with ammonia in the presence of water increases further at 250–350 °C, and is practically complete above 250 °C.

The observation that the NH_3 breakthrough profile becomes steeper with increasing reduction temperature is in line with the effect of temperature on the rate of the reaction. However, an increase in the reduction temperature also increases the quantities of stored nitrates, which are being reduced by NH_3. This may be related to the involvement of nitrate species stored on Ba sites far away from Pt sites in the reduction process. Indeed, it has been suggested that nitrates adsorbed on Ba sites near Pt are more easily reduced than NO_x species adsorbed on Ba sites far away from Pt [29]. Accordingly, it may be speculated that at low temperatures, only nitrates stored on Ba sites close to Pt are reduced; on increasing reduction temperature, nitrates stored far away from Ba also are involved in the reduction process due to the increased mobility of such species (or of the reductant) with increasing temperature. This is in line with previous suggestions as the roles of the spillover of the reductant from the metal to Ba sites, the reverse spillover of NO_x to the metal, as well as the reduction of the stored NO_x on Pt–Ba/Al_2O_3 catalysts [17].

Our data demonstrate that ammonia is an effective reductant for stored NO_x. On decreasing reduction temperature, the reactivity of ammonia toward adsorbed nitrates decreases, so that at 150 °C, the efficiency of nitrate reduction efficiency, well below that of H_2, which at this low temperature remains very efficient in the reduction of stored nitrates. These data are in line with the results of NH_3-TPSR experiments showing negligible reactivity of ammonia below 130 °C.

3.4. Mechanistic aspects of nitrate reduction by H_2

Our data clearly demonstrate that the stored nitrates are easily reduced by H_2 at very low temperatures, starting at 60 °C, leading to the formation of ammonia. Moreover, ammonia itself exhibits significant activity in the reduction of the stored nitrates, but at higher temperatures compared with H_2 (above 130–140 °C vs 60 °C). Of note, complete selectivity to nitrogen is observed in this case. Accordingly, these data are consistent with the hypothesis that the formation of N_2 during the regeneration of LNTs by H_2 occurs via an in-series two-step pathway involving first the fast formation of ammonia on reaction of nitrates with H_2 [reaction (2)], followed by the slower reaction of the ammonia thus formed with the stored nitrates, leading to the selective formation of N_2 [reaction (5)]. The sum of reactions (2) and (5) leads to the overall stoichiometry for the reduction of nitrates by H_2 [reaction (3)].

The reduction of the stored nitrates with hydrogen to give ammonia [reaction (2)] is very fast and is observed at very low tem-

perature, slightly above the ambient temperature. The subsequent reaction of ammonia with the stored nitrates to give nitrogen is much slower and thus is rate-determining in the formation of nitrogen.

The mechanism of ammonia formation on reduction of the stored nitrates with H_2 (step 1) is not completely clear. As shown in previous work, a Pt-catalyzed pathway is likely operating in this step [16–18,22]. H_2, activated over the Pt sites, may reduce the stored nitrates directly to ammonia or, more likely, provoke the decomposition of nitrates to gaseous NO_x which are then reduced by H_2 to NH_3 over the Pt sites. Indeed, as shown previously, the reduction of NO by H_2 can be accomplished at temperatures as low as 60 °C over the same Pt–Ba/Al_2O_3 catalyst sample used in the present study [28]. Moreover, studies on the reduction of NO by H_2 over Pt have shown that the selectivity of the process depends on the relative surface concentrations of the N-, H-, and O-adsorbed entities, which in turn are governed by the operating conditions (and specifically by the H_2/NO ratio) [8,29]. In our case, the very high selectivity to ammonia seen at low temperatures suggests that high H/N and H/O ratios are attained locally on the catalyst surface where the reaction occurs, thus driving the selectivity to ammonia and water.

Once ammonia has been formed, it may react further with adsorbed nitrates. This reaction is very selective toward nitrogen, as clearly demonstrated by both the NH_3-TPSR and NH_3-ITRM data. It is noteworthy that the reaction of ammonia with NO_x obeys the stoichiometry of reaction (5), which does not involve gas-phase NO_x. As a matter of fact, through dedicated experiments, we analyzed the NO + NH_3 reaction over the same catalyst sample used in this study [30], and found that the NO + NH_3 reaction led to significant amounts of N_2O, in contrast to the nitrate + NH_3 reaction, which is highly selective to N_2 (see Figs. 2B and 5). In addition, we found that Pt was involved in the reaction of ammonia with the stored nitrates, because the reduction of nitrates (and also of nitrites) stored on Ba could not be accomplished by NH_3 over a Pt-free sample [30]. Pt could activate NH_3 and/or could favor nitrate decomposition. The mechanistic features of this reaction remain unclear; however, an intermediate species must be invoked that decomposes rapidly and selectively to N_2.

In summary, we have found clear evidence for the existence of an in-series two-step process for the reduction of nitrates with H_2 to give N_2. Step 1 is represented by the fast reaction of H_2 with the stored nitrates to give ammonia, and step 2 involves the subsequent slower reduction of nitrates to give nitrogen. Of note, under the experimental conditions used in the present study (i.e., nearly isothermal conditions with limited temperature changes on the lean–rich cycles), the reaction of ammonia with nitrates represents the major route for nitrogen formation.

The two-step pathway described above for nitrogen formation from adsorbed nitrates accounts for the temporal evolution of the product selectivity observed during H_2-ITRM experiments carried out at high temperature (above 200 °C), with nearly complete N_2 selectivity at the beginning of the reduction process, followed by ammonia formation (see Fig. 3). Two recent papers [22,23] proposed a simplified scheme able to explain both the very high N_2 selectivity and the temporal sequence of the products (first N_2 and then NH_3) observed at 300 °C during regeneration of a LNT catalyst with H_2. The authors described the presence of a localized regeneration front that travels along the trap during reduction. Nitrogen and ammonia are formed on the reaction of H_2 with nitrates, but the high efficiency of the NSR catalyst in converting NO_x mainly to N_2 is achieved, because ammonia reacts further with nitrates to produce N_2. Accordingly, only N_2 is found at the reactor outlet during the initial regeneration period; later, NH_3 breakthrough is observed due to the depletion of NO_x remaining in the bed, which is of insufficient amount to react with the NH_3 formed upstream.

Our data provide additional information on the mechanism involved in the regeneration of LNTs and on the role of ammonia in the process. We get a slightly different picture from that suggested in previous reports [22,23], as shown in Fig. 6, which shows the ongoing reduction process in the catalyst bed. The fast reduction step of the adsorbed nitrates by H_2 to give ammonia and the "plug-flow" behavior of the reactor imply the complete consumption of the reductant H_2 and formation of an H_2 front along the reactor axis. Accordingly, the trap is regenerated upstream of the H_2 front, whereas nitrates remain present downstream of the front. At any given point of the regeneration phase, different zones are present in the reactor: (i) an initial zone, upstream of the H_2 front (zone I), where the trap already has been regenerated on the reduction of nitrates by H_2 and the Ba storage sites have been restored; (ii) the zone corresponding to the development of the H_2 front (zone II), where the concentration of hydrogen decreases from the inlet value to almost zero due to its fast reaction with the stored nitrates, and ammonia formation occurs; (iii) a zone immediately downstream of the H_2 front (zone III) in which nitrates are present because of the complete H_2 consumption upstream (i.e., in zone II) and in which at sufficiently high temperature, these nitrates react with ammonia formed upstream (zone II), leading to nitrogen formation; and (iv) the last zone (zone IV), in which the initial nitrates loading is still present. Notably, the spatiotemporal H_2 concentration profile inside the reactor is complex, resulting from the H_2 consumption leading to the formation of ammonia and from the depletion of adsorbed nitrates downstream of the H_2 front due to their reaction with ammonia (at high temperatures). But these phenomena result in similar H_2 concentration profiles at the reactor outlet at the different temperatures investigated (see Fig. 3).

The in-series two-step pathway suggested above for nitrogen formation, together with the integral nature of the regenerating trap, well explains the changes in the product distribution and the increased N_2 selectivity observed with temperature (Fig. 4B). When the regeneration of the trap is carried out at low temperatures (i.e., 150 °C or lower), H_2 reacts with surface nitrates to give NH_3 according to reaction (2), and the H_2 front develops (zone II). But due to the low temperature, ammonia can hardly react with the stored nitrates to form N_2 according to reaction (5), for which a temperature threshold of 130 °C was measured. As a result, ammonia is the major reaction product by far, and the nitrogen selectivity is very small. The negligible reactivity of ammonia toward nitrates at low temperature in the presence of H_2 also was confirmed by dedicated ITRM runs carried out with $NH_3 + H_2$ mixtures (results not shown).

On increasing reduction temperature, the reactivity of NH_3 with nitrates [reaction (5)] becomes appreciable, which drives the selectivity to N_2. Because H_2 is far more reactive than NH_3 toward surface nitrates, NH_3 reacts preferentially with nitrates located downstream of the H_2 front (i.e., in zone III of Fig. 6), leading to nitrogen formation. Accordingly, N_2 is observed first at the reactor outlet (Fig. 3), and the selectivity to N_2 increases (Fig. 4B).

Finally, at the highest temperatures investigated (e.g., 350 °C; Fig. 3), NH_3 readily reacts with the adsorbed NO_x [reaction (5)] even in the presence of H_2. This was demonstrated by dedicated ITRM experiments with $H_2 + NH_3$ mixtures (results not reported for the sake of brevity) showing that at high temperatures, NH_3 effectively competes with H_2 for reduction of the stored nitrates. Accordingly at high temperatures, the evolution of NH_3 at the reactor outlet is of only minor relevance, being readily consumed by the reaction with stored nitrates.

In conclusion, according to this picture, nitrogen formation is related to an in-series two-step process involving the intermediacy of ammonia. The first step of this in-series process (ammonia formation from H_2 + nitrates) is much faster than the second step

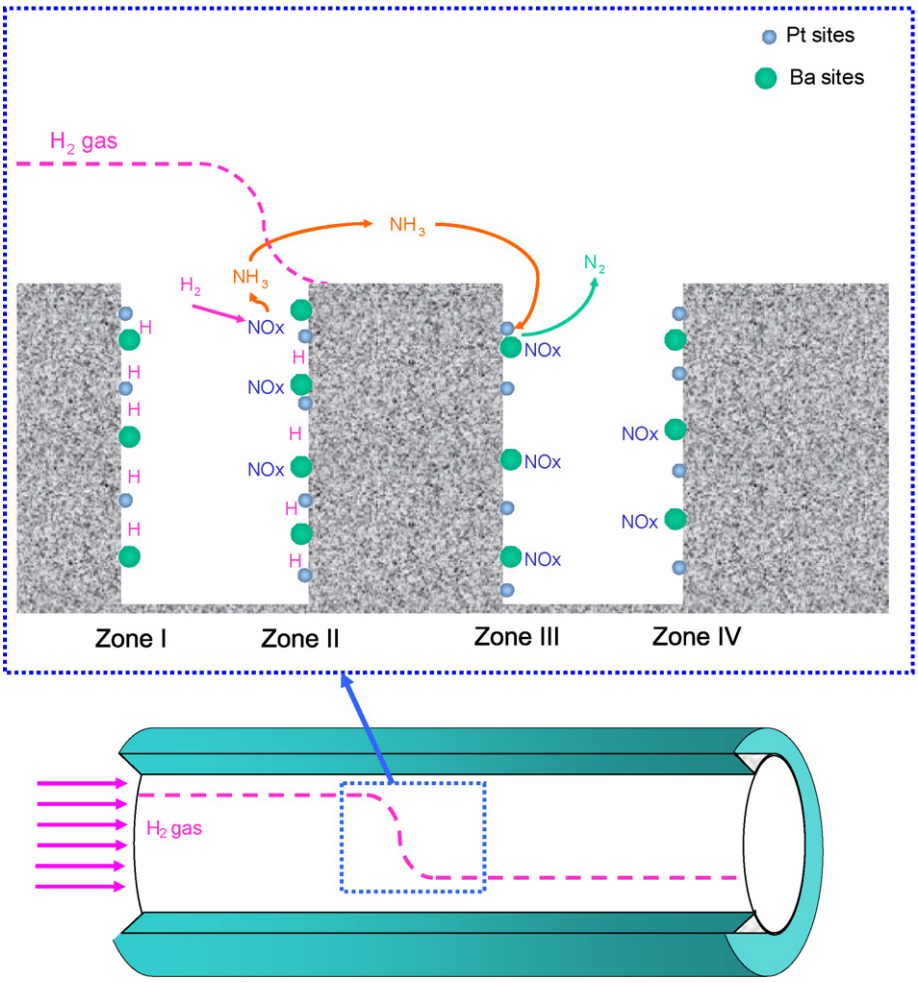

Fig. 6. Sketch of the reduction mechanism for a Pt–Ba/γ-Al_2O_3 catalyst upon regeneration with H_2.

(nitrogen formation on reaction of nitrates with NH_3). Accordingly, regeneration of the trap proceeds both in the part of the reactor in which nitrates are reduced by H_2 to give ammonia (zone II) and in the zone in which the ammonia formed upstream reacts with nitrates leading to N_2 (zones II and III). Moreover, the stoichiometry of the reaction between ammonia and stored nitrates is clearly identified [reaction (5)].

3.5. Effect of water on the reduction of stored nitrates

The H_2- and NH_3-TPSR and -ITRM experiments discussed so far were performed in the presence of water (1% v/v) in the feed stream. To address the effect of water on the reduction of the stored nitrates, we performed the same experiments in a water-free environment. Fig. 7 shows the results obtained from the TPSR experiments performed with H_2 and NH_3 under dry conditions.

In the H_2-TPSR experiment (Fig. 7A), the temperature threshold for hydrogen consumption is seen near 150 °C, well above that observed in the experiment carried out under wet conditions (50 °C; see Fig. 2A). The H_2 concentration shows a minimum of few tenths of ppm near 200 °C and then increases with temperature up to the inlet concentration value. Nitrogen is formed above 180 °C, showing a sharp peak with maximum near 200 °C. Ammonia formation also is evident above 185 °C, with a maximum near 220 °C. No other reaction products (e.g., NO, N_2O) are formed except for water (not shown in the figure), the evolution of which demonstrates a delay, possibly due to its adsorption on the regenerated BaO sites, with formation of $Ba(OH)_2$ according to reaction (4). Comparing this TPSR experiment with the analogous run carried out in the presence of water (Fig. 2A) indicates that water has a significant affect on the reduction of the stored nitrates by H_2, because the presence of water significantly decreases the temperature of onset of the reaction (2).

We also carried out reduction of the stored nitrates with H_2 at constant temperature (150–350 °C) under dry conditions after adsorption of NO_x at 350 °C. The results are displayed in Fig. 8, wherein concentration profiles of hydrogen, nitrogen, and ammonia measured at the reactor outlet are shown. In the experiment carried out at 150 °C, the reaction shows a significant induction period. Indeed, H_2 initially is detected unconverted at the reactor outlet; then, after 200 s, the H_2 concentration starts to decrease, reaching a minimum near 450–750 s. This decreased H_2 concentration is accompanied by the evolution of NH_3 and of minor amounts of N_2; however, a delay between NH_3 (and N_2) evolution (near 450 s) and H_2 uptake (200 s) is seen. As discussed earlier for the experiments carried out in the presence of water, this finding may indicate initial adsorption and activation of H_2 on the catalyst surface.

As shown in Fig. 4A, the regeneration of the catalyst is not complete at this temperature. Indeed, only 80% of the initially adsorbed NO_x could be reduced after prolonged treatment with H_2 at 150 °C. In addition, the overall N_2 selectivity is very poor, <20% (Fig. 4B).

When the reaction temperature is increased to 200 °C, the induction period almost disappears, and a small, sharp H_2 peak is observed on admission of H_2 to the reactor. N_2 formation is observed after the H_2 peak, followed by NH_3 evolution, which occurs

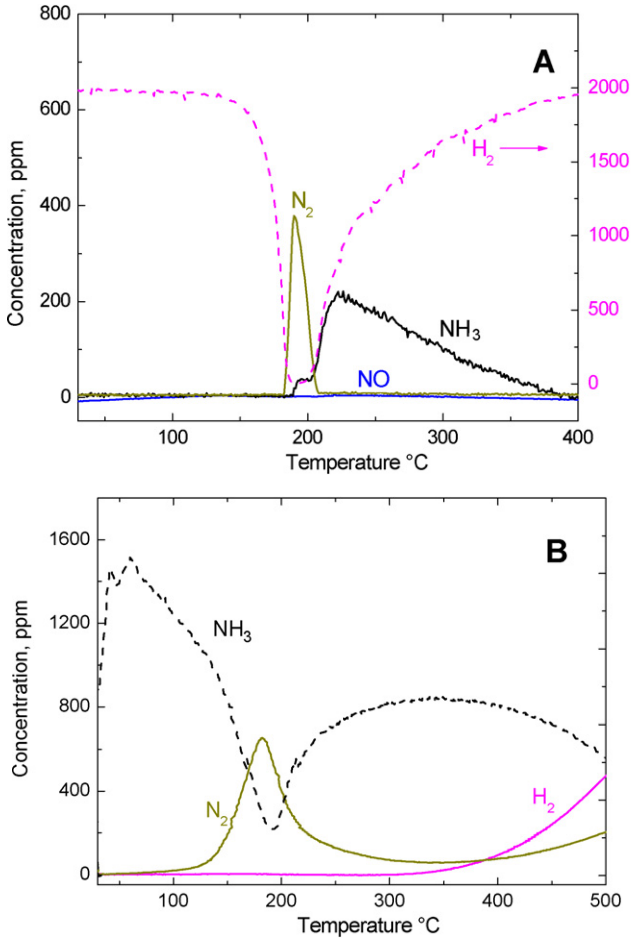

Fig. 7. H_2-TPSR (2000 ppm in He) (A) and NH_3-TPSR (1000 ppm in He) (B) after NO/O_2 adsorption at 350 °C over the Pt–Ba/γ-Al_2O_3 catalyst.

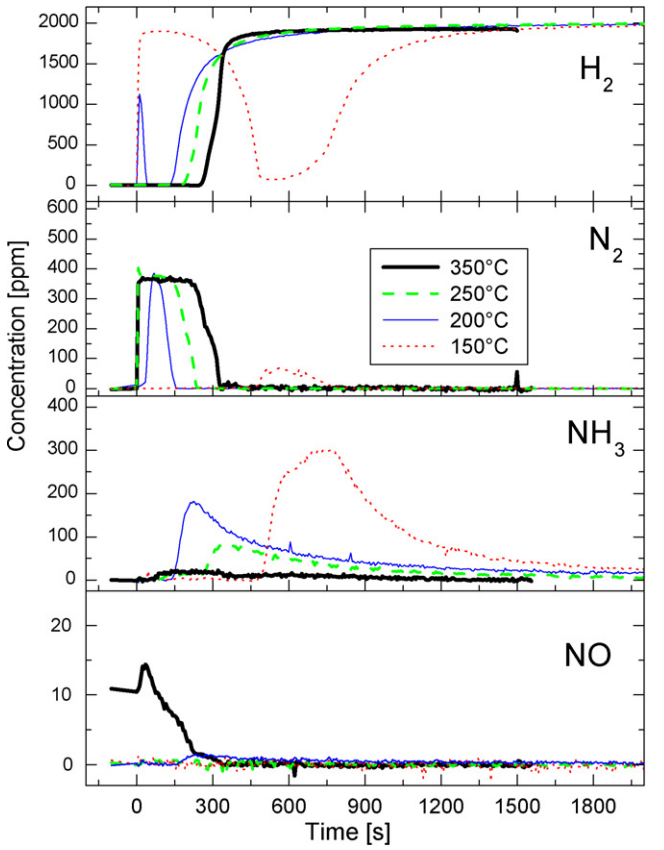

Fig. 8. Temporal evolution of H_2, N_2, NH_3 and NO outlet concentrations during reduction with H_2 (2000 ppm in He) after NO/O_2 adsorption at 350 °C over the Pt–Ba/γ-Al_2O_3 catalyst (H_2-ITRM experiment).

in concert with the H_2 breakthrough. On further increasing the reduction temperature, the initial H_2 peak disappears, and N_2 formation is seen immediately on the addition of H_2. The evolution of ammonia always follows that of N_2 and is accompanied by the detection of unconverted H_2. NH_3 formation decreases significantly with temperature, so that at the maximum investigated temperature (350 °C), only minor amounts of ammonia are detected. This leads to a significant increase in the selectivity of the reaction with temperature (see Fig. 4B).

Comparing the H_2-ITRM experiments performed in the absence of water (Fig. 8) with those carried out in the presence of water (Fig. 3) demonstrates that above 250 °C, the presence of water does not significantly affect the reduction process. In fact, the NO_x reduction efficiency and the N_2 selectivity are very similar at 250–350 °C (see Fig. 4). In contrast, the presence of water significantly affects the reduction process at lower temperatures; in the absence of water below 250 °C, the NO_x reduction efficiency decreases, and an induction period in the reduction of stored nitrates becomes apparent. This is particularly evident at 150 °C, where a very long induction period (in the order of several minutes) in the consumption of H_2 is seen. All of these observations indicate that water favors the reduction of stored nitrates by H_2.

We also analyzed the effect of water on the reactivity of NH_3 with nitrates. The results of the TPSR run carried out in the absence of water in the feed stream are shown in Fig. 7B. The NH_3 concentration profile exhibits complex behavior, with desorption at low temperature and consumption at higher temperatures. N_2 formation is apparent above 120–130 °C, with a maximum near 180 °C; the formation of no other reaction products is observed. At high temperatures (above 350 °C), the formation of N_2 and H_2 also is observed, due to ammonia decomposition.

The NH_3-TPSR experiment carried out in the presence of water (Fig. 2B) shows similar concentration profiles of N_2 and H_2 versus temperature; only a small shift towards higher temperatures is observed. On the other hand, the NH_3 concentration profile is different, because the low-temperature NH_3 desorption peak is not observed in the presence of water. This effect is related to the competitive adsorption of water and ammonia on the catalyst surface, with water displacing ammonia from the catalyst adsorption sites in view of its much greater concentration level (10.000 ppm vs 1000 ppm).

In summary, the NH_3-TPSR data demonstrate that water only slightly inhibits the reactivity of ammonia in the reduction of the stored nitrates, opposite to what occurs in the case of H_2. This also has been confirmed by NH_3-ITRM experiments (not reported here for brevity) showing results very similar to those obtained in the presence of water (Fig. 5).

The foregoing data indicate that water clearly favors the first step of the reduction process (reduction of nitrates to give ammonia) but has no significant impact on the subsequent step (reaction of ammonia with the stored nitrates). Indeed, in the presence of water, nitrates are reduced by H_2 at lower temperatures, at which ammonia is not effective as a reductant. This favors the reduction of the stored NO_x to give NH_3, thus favoring the selectivity to ammonia at low temperatures, explaining the higher amounts of ammonia seen during the H_2-TPSR run carried out in the presence of water compared with the analogous run carried out in a dry environment (compare Figs. 2A and 7A).

It can be speculated that water favors H_2 spillover, which is considered an important step in the reduction of the stored ni-

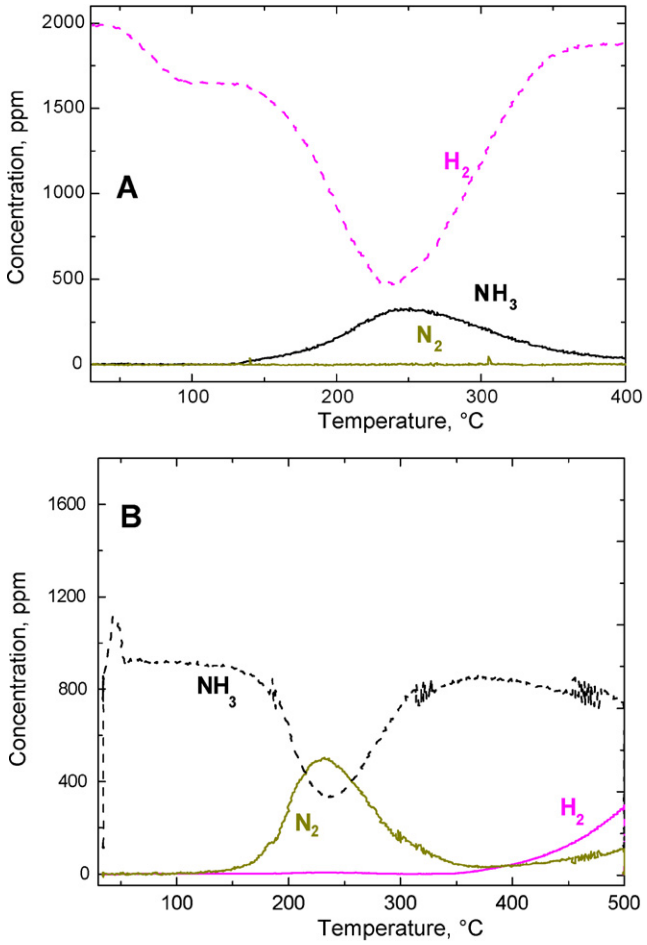

Fig. 9. H_2-TPSR (2000 ppm + 1% v/v H_2O + 0.3% v/v CO_2 in He) (A) and NH_3-TPSR (1000 ppm + 1% v/v H_2O + 0.3% v/v CO_2 in He) (B) after NO/O_2 adsorption at 350 °C over the Pt–Ba/γ-Al_2O_3 catalyst.

trates [18,19]. This should increase the rate of nitrate reduction, as indeed has been observed in H_2-ITRM experiments, in which the presence of water significantly decreases the induction time of the reaction. As a matter of fact, several literature reports indicate that water increases the H_2 spillover rate over oxidic surfaces [31]. In this case, a significantly enhanced reduction of nitrates stored far away from Pt sites, whose reaction implies the mobility of H adspecies on the surface, can be expected. Specific effects of water on the mobility of adsorbed nitrates, which also may play a role in the reaction, also can be suggested, but this is expected to play only a minor role at low temperatures, where the promoting effect of water is well evident. Finally, it is noteworthy that water also affects the features of nitrate adspecies, as reported recently [32] and also demonstrated by dedicated FTIR experiments carried out in our lab [30]. Interestingly, water affects the reactivity of H_2 with nitrates but has no significant effect toward NH_3; the negligible impact of H_2O on the reactivity of ammonia with nitrates is in line with the fact that NH_3 activation occurs on Pt sites, as discussed previously, and that water does not significantly affect this step. These points require further clarification, however.

3.6. *Effect of CO_2 on the reduction of stored nitrates*

Finally, we investigated the effect of the presence of carbon dioxide on the reduction of the stored nitrates. For this purpose, TPSR and ITRM runs were performed in the presence of water (1% v/v) and CO_2 (3000 ppm). The results are shown in Figs. 9 and 10.

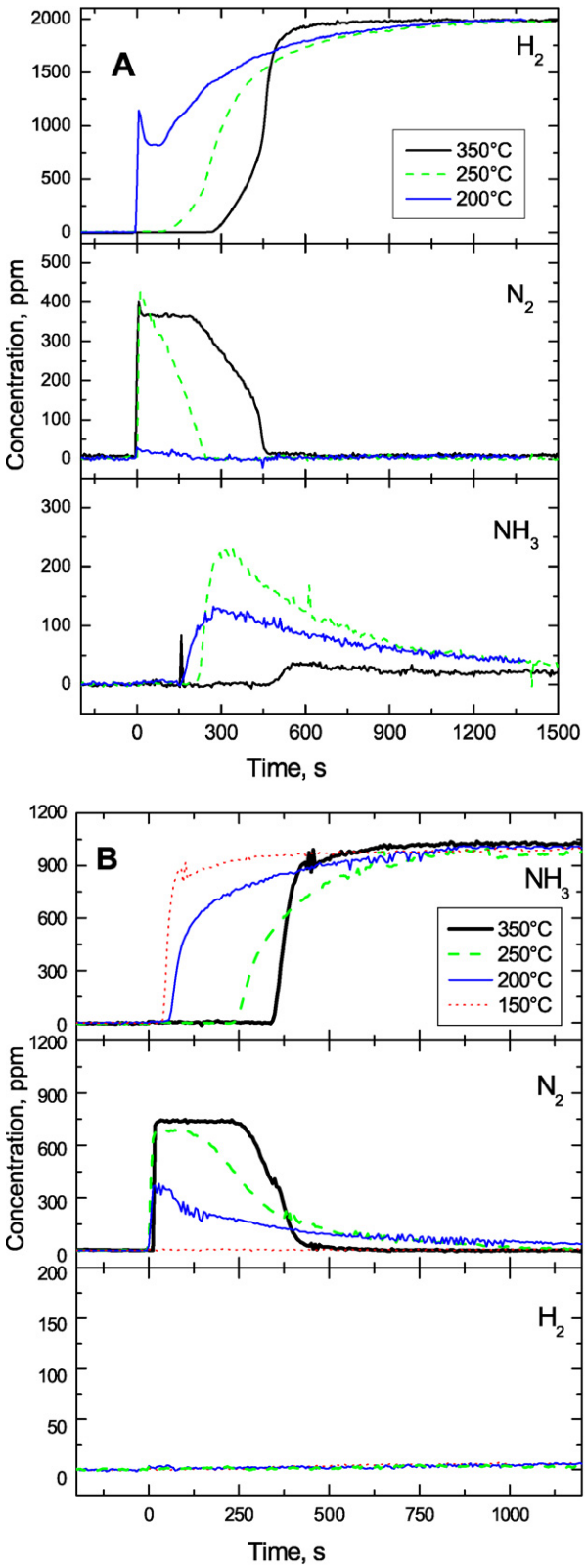

Fig. 10. Temporal evolution of H_2, N_2 and NH_3 outlet concentrations during reduction with H_2 (2000 ppm + 1% v/v H_2O + 0.3% v/v CO_2 in He) (A) and with NH_3 (1000 ppm + 1% v/v H_2O + 0.3% v/v CO_2 in He) (B) after NO/O_2 adsorption at 350 °C over the Pt–Ba/γ-Al_2O_3 catalyst.

In the H_2-TPSR experiment (Fig. 9A), hydrogen shows a consumption peak with a minimum near 230 °C, accompanied by the formation of ammonia. An H_2 uptake with a shoulder in the low-temperature region also is seen, which, however, does not cor-

respond to any release of reaction products. Formation of N_2 is negligible during the whole run. No appreciable formation of CO is observed in the high-temperature region, as might be expected due to the reverse water–gas shift reaction (WGSR),

$$CO_2 + H_2 \rightarrow CO + H_2O. \quad (7)$$

It is noteworthy that CO formation occurs above 300 °C during the TPSR experiments carried out in the absence of water in the feed stream (data not shown). This indicates that water present in the feed stream (1% v/v) drives reaction (7) (which is near chemical equilibrium at 400 °C) from right to left.

A comparison with an analogous TPSR run performed in a CO_2-free environment (Fig. 2A) clearly demonstrates that CO_2 has a strong inhibiting effect on the reduction of the stored nitrates by H_2, with a maximum effect in the formation of ammonia (and the corresponding H_2 consumption peak) shifted at higher temperature by nearly 150 °C, from 100 to 250 °C. A possible explanation for this inhibiting effect of CO_2 is related to poisoning of the Pt sites by carbonyls formed on the reduction of CO_2 by H_2 (i.e., according to the reverse WGSR). This reaction can occur to a limited extent already at low temperatures, as demonstrated by our previous dedicated FTIR experiments carried out over the same catalyst sample indicating that Pt-carbonyls can be formed at temperatures as low as 150 °C in the presence of a CO_2/H_2 mixture, although CO is not detected in significant amounts in the gas phase [30]. Thus, the features of the TPSR experiment shown in Fig. 9A can be explained by considering that H_2 is initially adsorbed on the catalyst surface, thus accounting for the H_2 uptake at low temperatures. At higher temperatures, the Pt sites become blocked by CO (not detectable in the gas phase due to its low concentration) formed on CO_2 reduction. This shifts the reactivity toward higher temperatures, above those corresponding to the decomposition of the Pt carbonyls due to the occurrence of the WGSR. Indeed, in the presence of CO_2 in the feed stream but in the absence of water, the reduction of the stored nitrates is shifted at even higher temperatures, above 180 °C (data not shown). The participation of isocianate species in the reaction cannot be excluded in this case, as was suggested by Lesage et al. [33] and by Szailer et al. [32].

To investigate this possible explanation, we performed H_2-TPSR experiments with H_2/H_2O in the absence of CO_2 but the presence of small amounts of CO (100 ppm). The results (not reported for the sake of brevity) demonstrate that the presence of CO shifts the onset of the reaction to higher temperatures compared with that in a CO-free environment (160 °C vs 60 °C). Of note, the presence of CO_2 shifts the onset of the reaction (Fig. 9A) at the same temperature observed in the presence of CO (160 °C). This is in line with the hypothesis that Pt sites are blocked by CO, inhibiting the reaction.

Fig. 10A shows the results of the H_2-ITRM experiments carried out at different temperatures (at 150–350 °C) in the presence of water and CO_2 and after NO_x adsorption at 350 °C. The figure displays concentration profiles of hydrogen, nitrogen, and ammonia measured at the reactor outlet as a function of time.

In the experiment carried out at 200 °C, H_2 is only partially consumed after admission. The formation of ammonia is observed with a delay of about 150 s, whereas no N_2 is formed at these temperatures. A comparison with the run carried out at the same temperature in the absence of CO_2 (Fig. 3) confirms the very strong inhibiting effect of CO_2 on the reduction of the stored nitrates. Indeed, close to 50% of the stored NO_x is reduced in the presence of CO_2 at 200 °C (Fig. 4A), whereas complete NO_x reduction occurs in the absence of CO_2.

On increasing the reaction temperature to 250 °C, on step admission, H_2 is completely consumed and N_2 formation is observed, followed by NH_3 evolution. Nonetheless, the reaction is slightly inhibited by CO_2 at this temperature, as indicated by the slightly less efficient reduction of the stored NO_x (see Fig. 4A). The effect of CO_2 tends to vanish at the highest investigated temperature (350 °C), where very similar concentration profiles versus time are obtained in the presence and in the absence of CO_2 (compare Figs. 10A and 3). No appreciable CO formation is seen during the H_2-ITRM experiments, for the reasons discussed above.

We also analyzed the effect of CO_2 on the reactivity of NH_3 with the stored nitrates by TPSR and ITRM experiments; the results are shown in Figs. 9B (TPSR) and 10B (ITRM). In the TPSR experiment (Fig. 9B), a NH_3 consumption peak is seen starting near 150 °C, with a minimum at 240 °C. A corresponding evolution of nitrogen is observed, the concentration of which obeys the stoichiometry of reaction (5). At high temperatures (above 350 °C), H_2 and N_2 formation occur due to the NH_3 decomposition reaction.

Comparing these findings with those of the analogous TPSR experiment carried out in the absence of CO_2 (see Fig. 2B) demonstrates that the presence of carbon dioxide inhibits the reactivity of ammonia with stored nitrates, because the NH_3 consumption peak (and the corresponding N_2 evolution) is shifted to higher temperatures by 30–40 °C. Nonetheless, only N_2 is detected among the reaction products, as in the case of the CO_2-free experiments.

The fact that Pt is involved in the reaction of NH_3 with the stored nitrates, as discussed previously, suggests that the observed inhibiting effects of CO_2 on the NH_3 + nitrate reaction are related (as in the case of the reduction with H_2) to the poisoning of Pt by CO formed on the reduction of CO_2 on Pt sites reduced by NH_3. Of note, comparing Figs. 9A and 9B clearly shows that the temperature threshold for NH_3 formation in the H_2-TPSR experiments corresponds to the temperature threshold for N_2 formation in the NH_3-TPSR experiments. This suggests that in both cases, the reaction is limited by the reactivity of Pt sites, which are poisoned by CO. Once CO is removed from the Pt sites (via the WGSR), both H_2 and NH_3 react with the stored NO_x. Of note, the decomposition of Pt carbonyls is favored by the presence of water (i.e., the inhibiting effect of CO_2 is of lower importance in a dry environment), as confirmed by experiments carried out with CO_2 in the absence of water (data not shown).

Finally, we investigated the effect of CO_2 on the reactivity of ammonia with the stored nitrates through NH_3-ITRM experiments performed at various temperatures in the presence of CO_2 and water. The results, shown in Fig. 10B, indicate that at 150 °C, the reactivity of ammonia is negligible; in fact, <10% of the initially adsorbed NO_x is reduced at this temperature. The reaction occurs starting at 200 °C, with formation of small amounts of N_2 after the admission of NH_3 to the reactor. The overall N_2 production corresponds to a <70% reduction in the NO_x adsorbed initially. On increasing reaction temperature, N_2 formation is increased (as is the efficiency of the reduction of the stored NO_x), so that complete NO_x reduction is achieved at 350 °C. Comparing these data with the results of NH_3-ITRM experiments performed in the absence of CO_2 (Fig. 5) confirms the inhibiting effect of CO_2 on the reactivity of ammonia with stored nitrates. Indeed, in the absence of CO_2, complete and efficient reduction of the stored NO_x by NH_3 can be obtained already at 250 °C, whereas in the presence of CO_2, complete nitrate reduction is seen only above 300 °C. Moreover, N_2 is the sole reaction product in this case.

Based on the foregoing data, following the in-series two-step pathway previously proposed for the reduction of nitrates to N_2, the presence of CO_2 clearly inhibits both the initial reduction of nitrates to ammonia by H_2 and the subsequent reaction of ammonia with the stored nitrates, due to the poisoning of Pt by CO (formed via the reverse WGSR). Accordingly, in the reduction of the stored nitrates with H_2, the presence of CO_2 leads to both lower efficiency in the reduction of the stored NO_x (due to inhibition of the first step of nitrate reduction) and higher selectivity to ammonia at low

temperatures (due to inhibition of CO_2 on the subsequent reaction of ammonia with nitrates).

4. Conclusion

In this study, we investigated the reduction by H_2 of nitrates stored on a model Pt–Ba/Al_2O_3 catalyst sample. An in-series two-step pathway for nitrogen formation involving the fast formation of ammonia on reaction of nitrates with H_2 [reaction (2)], followed by the slower reaction of the ammonia thus formed with the stored nitrates leading to the selective formation of N_2 [reaction (5)] is proposed:

$$Ba(NO_3)_2 + 8H_2 \rightarrow 2NH_3 + Ba(OH)_2 + 4H_2O, \quad (2)$$

$$3Ba(NO_3)_2 + 10NH_3 \rightarrow 8N_2 + 3Ba(OH)_2 + 12H_2O. \quad (5)$$

The sum of reactions (2) and (5) leads to the overall stoichiometry for the reduction of nitrates by H_2,

$$Ba(NO_3)_2 + 5H_2 \rightarrow N_2 + Ba(OH)_2 + 4H_2O. \quad (3)$$

This proposed in-series two-step pathway is based on the observation that in the presence of water, nitrates are readily reduced by H_2 at very low temperatures, starting at 60 °C, leading to the selective formation of ammonia, which in turn selectively reduces nitrates to N_2 but at higher temperatures compared with those for the reduction of H_2. Indeed, different temperature thresholds for these two steps are clearly identified (130–140 °C vs 60 °C), with step 1 (reduction of the stored nitrates to give ammonia) being much faster than step 2 (formation of nitrogen by reaction of ammonia with nitrates). Consequently, step 2 is rate-determining in the formation of nitrogen, so that under the present experimental conditions (i.e., nearly isothermal conditions with limited temperature excursions during cycling), the reaction of ammonia with nitrates represents the major route of nitrogen formation.

Ammonia formation on reduction of the stored nitrates with H_2 (step 1) likely occurs via a mechanism that involves the activation of H_2 over Pt sites, followed by decomposition of nitrates to gaseous NO_x, which eventually is reduced by H_2 over the Pt sites. Almost complete selectivity to ammonia is observed in this case, due to the high H/N ratio attained locally on the catalyst surface where the reaction occurs. Once ammonia is formed, it may react further with adsorbed nitrates; this reaction is very selective toward nitrogen. The stoichiometry of this reaction has been clearly identified [i.e., reaction (5)]. It also has been found that Pt is necessary for the reaction of ammonia with the stored nitrates, which may suggest the involvement of Pt in the activation of ammonia.

The in-series two-step pathway described herein is able to account for the temporal evolution of the product selectivity observed during regeneration of LNT catalysts. Indeed, at high temperatures, the fast reduction step of the adsorbed nitrates by H_2 to give ammonia, along with the integral "plug-flow" behavior of the reactor, imply complete consumption of the reductant H_2 and formation of an H_2 front along the reactor axis. Accordingly, the efficiency in the reduction of the stored NO_x is almost complete. Ammonia is readily formed on reaction of H_2 with the stored nitrates; at sufficiently high temperatures, ammonia reacts with nitrates remaining downstream of the H_2 front [reaction (5)] or even competes with H_2 for the reduction of nitrates upstream of the H_2 front. This drives the selectivity to N_2, which is found at the reactor outlet; the NH_3 breakthrough is seen together or after the H_2 breakthrough (i.e., when the H_2 front reaches the end of the trap).

At low temperatures, the rate of NO_x reduction by H_2 to give ammonia slows, the hydrogen front is less steep, and the reduction of stored nitrates by ammonia is significantly slower. Together, these effects limit the efficient reduction of the stored NO_x with low nitrogen selectivity, and, consequently, the breakthrough of NH_3 precedes that of H_2.

Water and CO_2 have significant effects on the reduction process. In particular, water favors the first step of the process (reduction of nitrates to ammonia) but has no significant affect on the subsequent reaction of ammonia with the stored nitrates. Accordingly, when the regeneration of the LNT catalyst is carried out in a dry environment, the reactivity of nitrates with H_2 shifts to higher temperatures, in the same range at which ammonia reacts with nitrates. In line with previous reports [31], it can be suggested that water favors H_2 spillover, thereby increasing the rate of nitrate reduction by H_2 (i.e., ammonia formation), but water also likely affects the features of nitrates adspecies. On the other hand, the negligible impact of H_2O on the reactivity of ammonia with nitrates is in line with the fact that Pt participates in the reaction by activating NH_3 (and/or favoring nitrate decomposition), a step unaffected by the presence of water.

Finally, we found that CO_2 inhibits both the initial reduction of nitrates to ammonia by H_2 (step 1) and the subsequent reaction of ammonia with the stored nitrates (step 2). The inhibition effect is due to the poisoning of Pt by CO, formed via the reverse WGSR, leading to the formation of Pt carbonyls. Accordingly, in the reduction of the stored nitrates with H_2, the presence of CO_2 leads to both lower efficiency in the reduction of the stored NO_x (due to the inhibition of the first step of nitrate reduction) and higher selectivity to ammonia at low temperatures (due to the inhibition of CO_2 on the subsequent reaction of ammonia with nitrates). The inhibition of CO_2 on reduction of the stored nitrates tends to vanish at high temperature due to the decomposition of Pt carbonyls, which is favored by the presence of water.

References

[1] P. Forzatti, L. Lietti, E. Tronconi, in: I.T. Horvath (Ed.), Nitrogen Oxides Removal—Industrial. Encyclopedia of Catalysis, first ed., Wiley, New York, 2002, and references therein.
[2] P.L.T. Gabrielsson, Top. Catal. 28 (2004) 177–184.
[3] M.A. Gómez-García, V. Pitchon, A. Kiennemann, Environ. Int. 31 (3) (2005) 445.
[4] I. Nova, C. Ciardelli, E. Tronconi, D. Chatterjee, M. Weibel, Top. Catal. 42–43 (1–4) (2007) 43–46.
[5] N. Miyoshi, S. Matsumoto, K. Katoh, T. Tanaka, J. Harada, N. Takahashi, K. Yokota, M. Sugiura, K. Kasahara, SAE technical paper 950809 (1995).
[6] S. Matsumoto, CATTECH 4 (2000) 102.
[7] Staff report, Modern Power Systems, March 2000, p. 23.
[8] W.S. Epling, L.E. Campbell, A. Yezerets, N.W. Currier, J.E. Park II, Catal. Rev. 46 (2004) 163.
[9] B. Konrad, B. Krutzsch, D. Voigtlaender, US patent US 6,176,079B1 (23.1.2001).
[10] K.S. Kabin, R.L. Muncrief, M.P. Harold, Catal. Today 96 (2004) 79–89.
[11] V. Medhekar, V. Balakotaiah, M.P. Harold, Catal. Today 121 (2007) 226.
[12] Z. Liu, J.A. Anderson, J. Catal. 224 (2004) 18.
[13] E. Fridell, M. Skoglundh, B. Westerberg, S. Johansson, G. Smedler, J. Catal. 183 (1999) 196.
[14] N.W. Cant, M.J. Patterson, Catal. Lett. 85 (2003) 153.
[15] S. Poulston, R. Rajaram, Catal. Today 81 (2003) 603.
[16] I. Nova, L. Lietti, L. Castoldi, E. Tronconi, P. Forzatti, J. Catal. 239 (2006) 244.
[17] N.W. Cant, I.O.Y. You, M.J. Patterson, J. Catal. 246 (2006) 309.
[18] J.R. Theis, H.W. Jen, R.W. McCabe, M. Sharma, V. Balakotaiah, M.P. Harold, SAE technical paper 2006-01-1067.
[19] M. Machida, D. Kurogi, T. Kijima, J. Phys. Chem. B 107 (2003) 196.
[20] R. Burch, J. Breen, F. Meunier, Appl. Catal. B Environ. 39 (2002) 283.
[21] T. Maunula, J. Ahola, H. Hamada, Appl. Catal. B Environ. 26 (2000) 173.
[22] L. Cumaranatunge, S.S. Mulla, A. Yezerets, N.W. Currier, W.N. Delgass, F.H. Ribeiro, J. Catal. 246 (2007) 29.
[23] J.A. Pihl, J.E. Parks II, C.S. Daw, T.W. Root, SAE technical paper, 2006-01-3441.
[24] L. Lietti, P. Forzatti, I. Nova, E. Tronconi, J. Catal. 204 (2001) 175.
[25] N. Miyoshi, T. Tanizawa, K. Kasahara, S. Tateishi, Eur. Patent Appl. 0 669 157 A1 (1995).
[26] I. Nova, L. Castoldi, F. Prinetto, G. Ghiotti, L. Lietti, E. Tronconi, P. Forzatti, J. Catal. 222/2 (2004) 377.
[27] I. Nova, L. Castoldi, F. Prinetto, V. Dal Santo, L. Lietti, E. Tronconi, P. Forzatti, G. Ghiotti, R. Psaro, S. Recchia, Top. Catal. 30/31 (2004) 181.
[28] I. Nova, L. Castoldi, L. Lietti, E. Tronconi, P. Forzatti, SAE technical paper, 2006-01-1368.

[29] Y. Sakamoto, K. Okumura, Y. Kizaki, S. Matsunaga, N. Takahashi, H. Shinjoh, J. Catal. 238 (2006) 361.
[30] Unpublished results from our Labs.
[31] M. Stoica, M. Caldararu, N.I. Ionescu, A. Auroux, Appl. Surf. Sci. 153 (2000) 218.
[32] T. Szailer, J.H. Kwak, D.H. Kim, J.C. Hanson, C.H.F. Peden, J. Szanyi, J. Catal. 239 (2006) 51.
[33] T. Lesage, C. Verrier, P. Bazin, J. Saussey, M. Daturi, Phys. Chem. Chem. Phys. 5 (2003) 4435.